

Electronic Supplementary Information

Altering Synthetic Fragments to Tune the AIE Properties and Self-assemble Grid-like Structures of TPE-based Oxacalixarenes

Zhen Wang,^{‡a} Hong Cheng,^{‡b} Tian-Long Zhai,^a Xianggao Meng*^c and Chun Zhang*^a

^a*College of Life Science and Technology, Huazhong University of Science and Technology, and National Engineering Research Center for Nanomedicine, Wuhan, 430074, China.*

^b*Analytical and Testing Center, Huazhong University of Science and Technology, Wuhan, 430074, China.*

^c*School of Chemistry, Central China Normal University, Wuhan 430079, China.*

Email: chunzhang@hust.edu.cn

1. ¹ H NMR and ¹³ C NMR spectra of 1a and 1b -----	S2
2. IR spectra of 1a and 1b -----	S4
3. Crystal structures of 1a -----	S5
4. Crystal structures of 1b -----	S5
5. The Self-assemblies of 1a in water/THF-----	S6
6. Fluorescent titration experiments of 1a -----	S7

1. ^1H NMR and ^{13}C NMR spectra of 1a and 1b

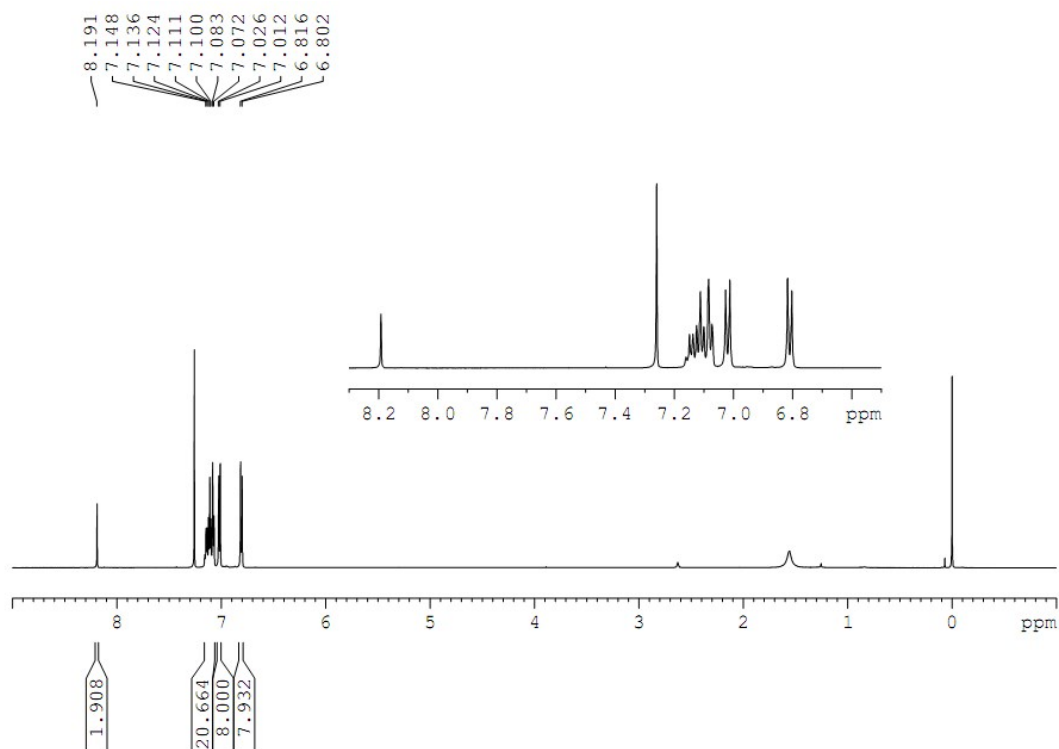


Fig. S1 ^1H NMR spectrum (600 MHz, CDCl_3) of 1a.

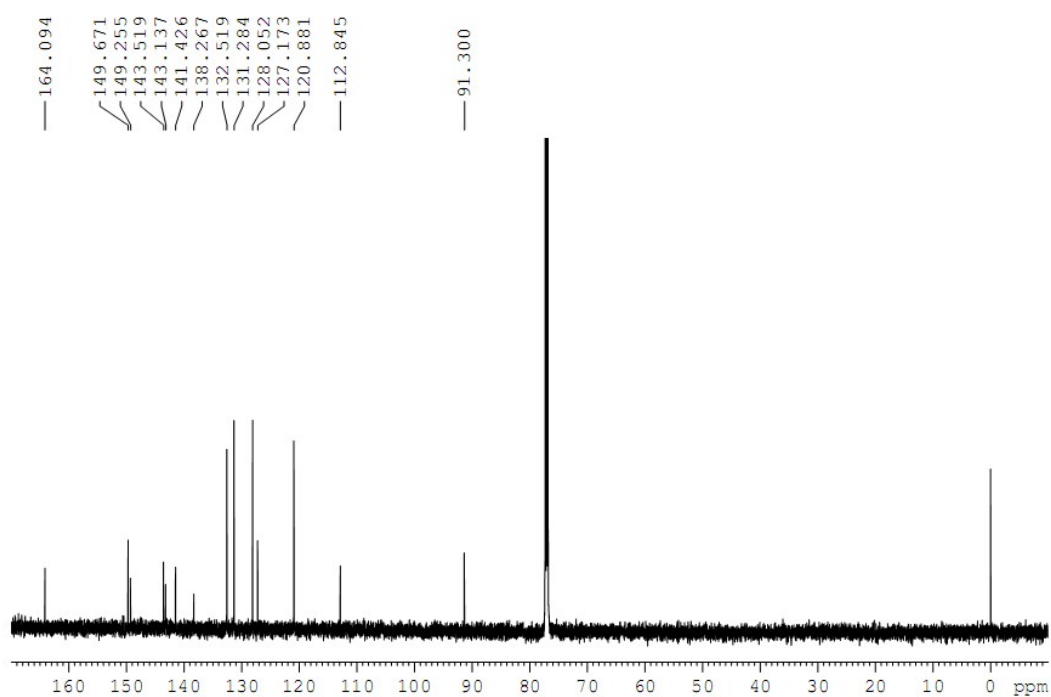


Fig. S2 ^{13}C NMR spectrum (150 MHz, CDCl_3) of 1a.

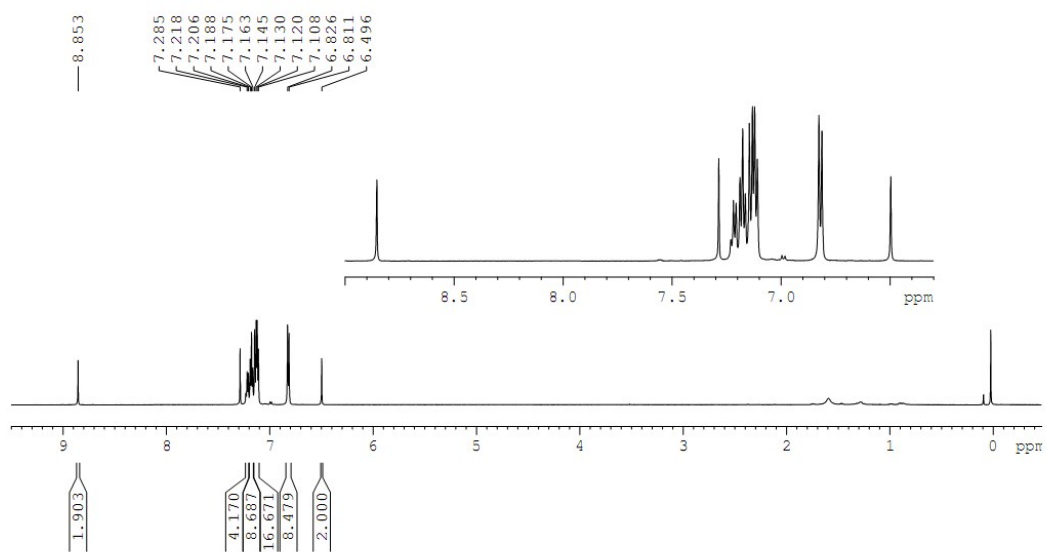


Fig. S3 ^1H NMR spectrum (600 MHz, CDCl_3) of **1b**.

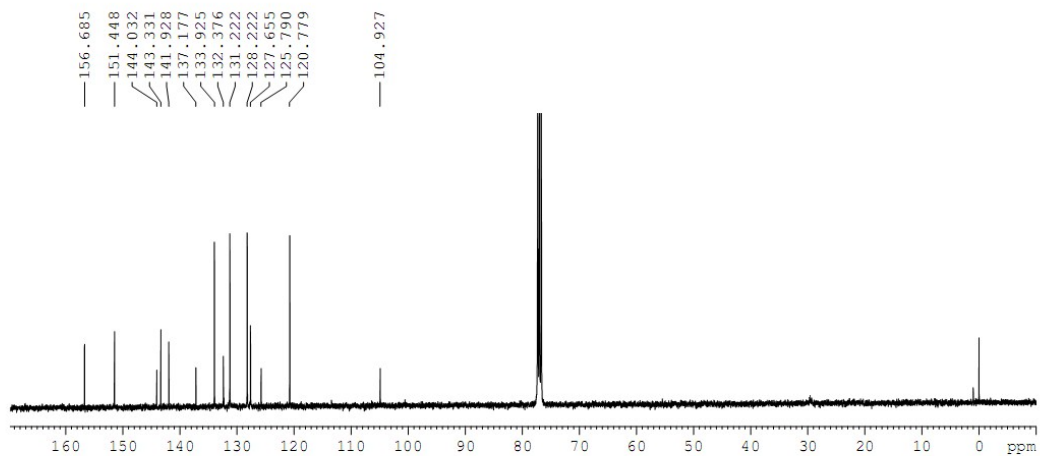


Fig. S4 ^{13}C NMR spectrum (150 MHz, CDCl_3) of **1b**.

2. IR spectra of 1a and 1b

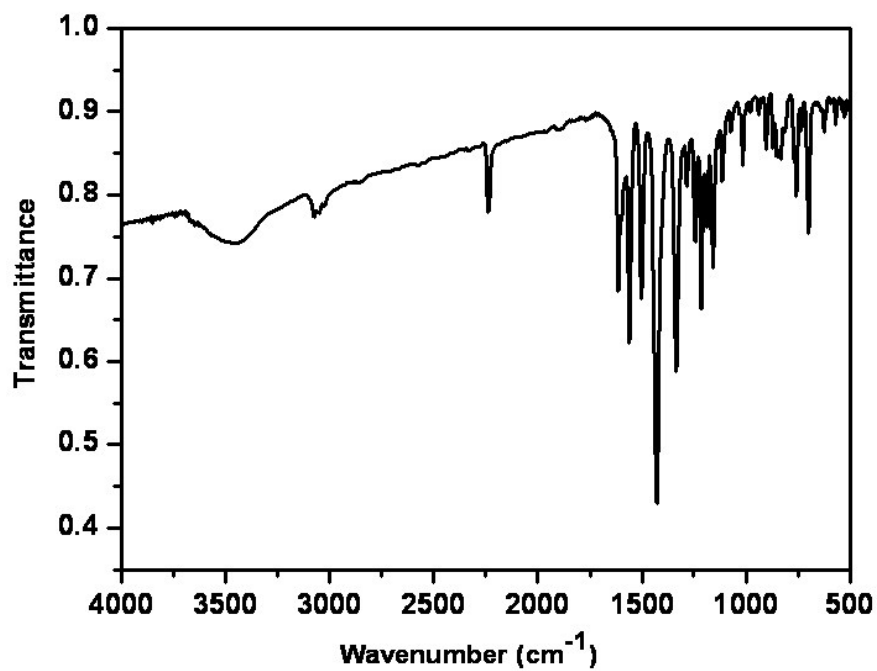


Fig. S5 IR spectrum of 1a.

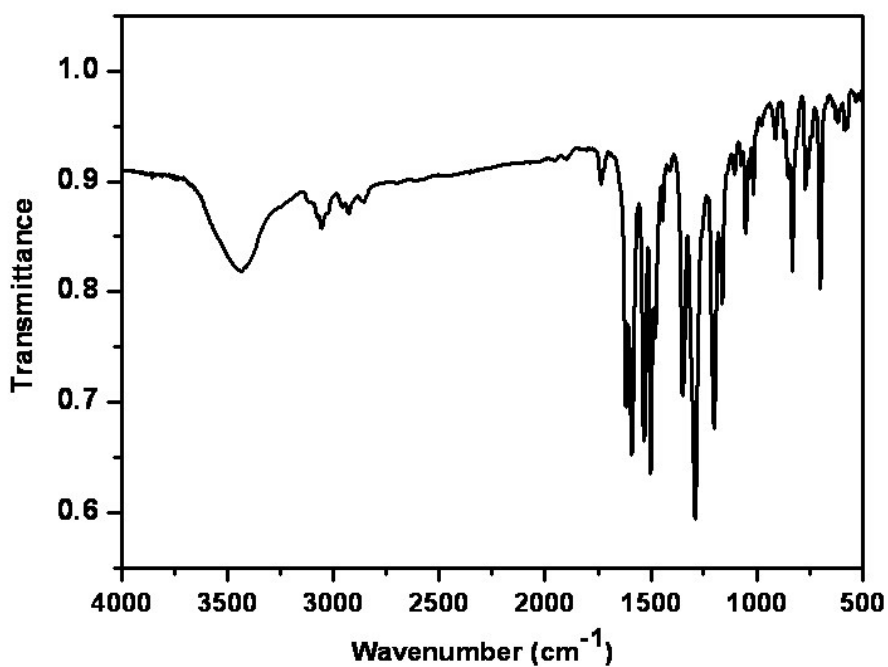


Fig. S6 IR spectrum of 1b.

3. Crystal structure of 1a.

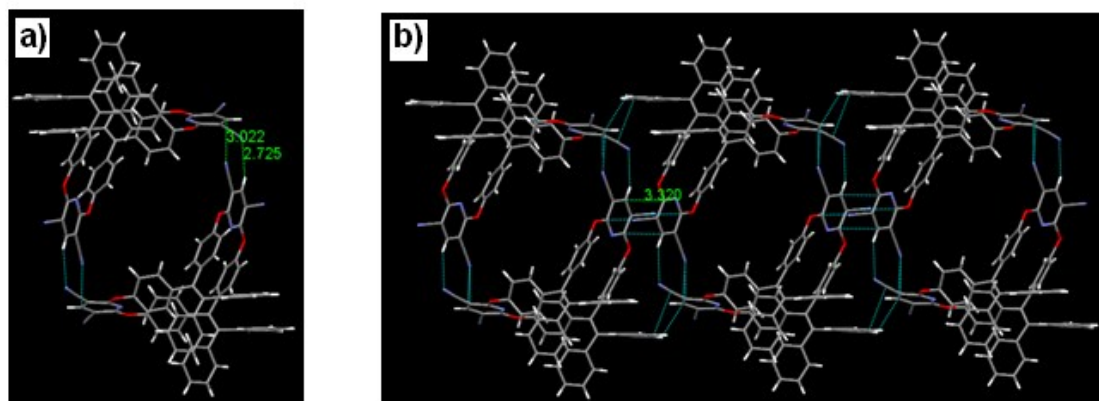


Fig.S7 The dimer structures (a), and one-dimensional linear grid structure (c) of oxacalixarene **1a**.

4. Crystal structure of 1b.

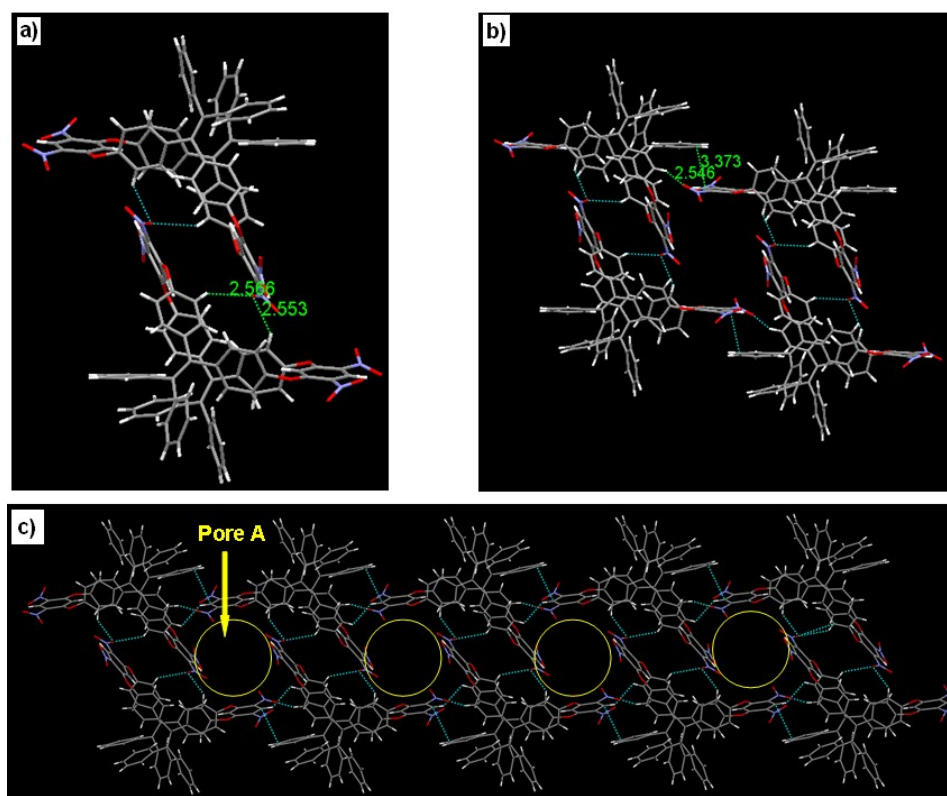


Fig. S8 The dimer structures (a), the grid-like pore A (b) and one-dimensional linear grid structure (c) of oxacalixarene **1b**.

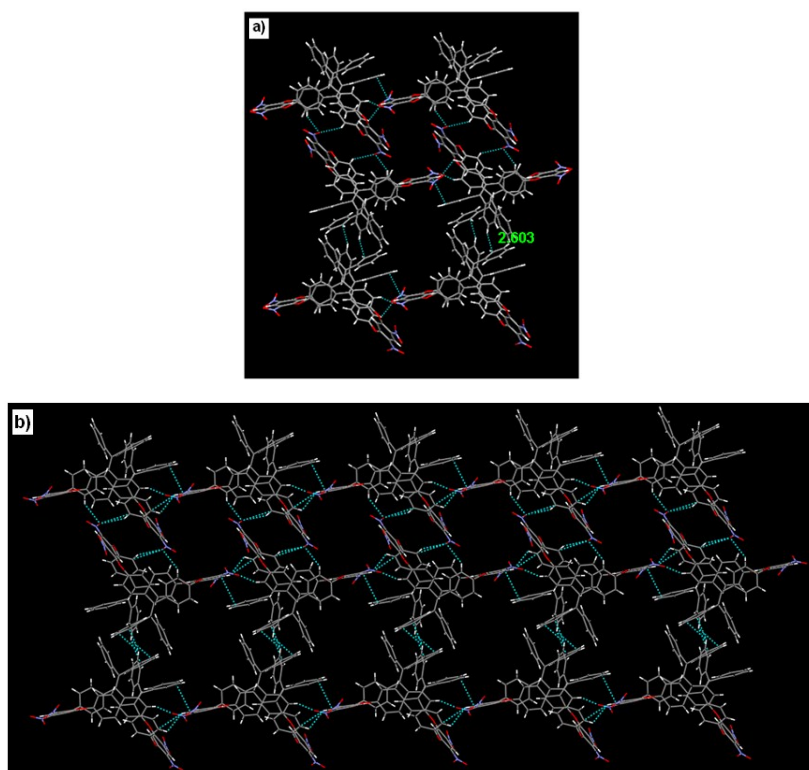


Fig. S9 The grid-like pore B (a) and two-dimensional grid structure (b) of oxacalixarene **1b**.

5. The Self-assemblies of **1a** in water/THF

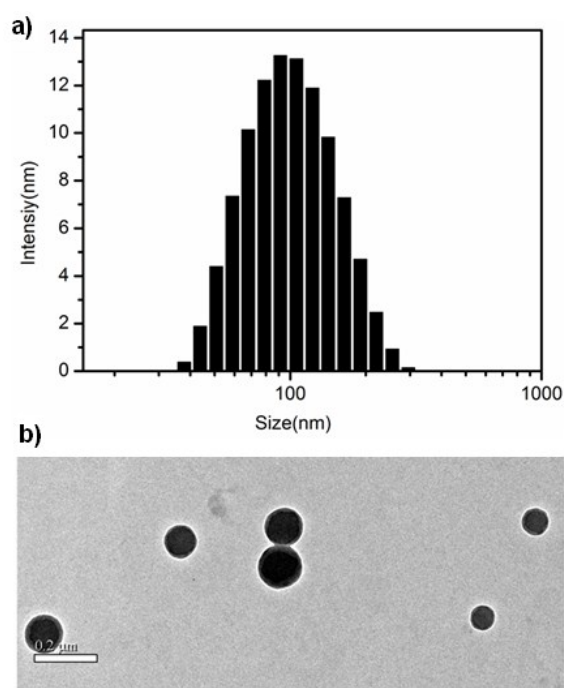


Fig.S10 The hydrodynamic size (a) and TEM image (b) of **1a** in water/THF (95/5) with concentration of 0.1 mg/mL.

6. The fluorescent titration experiments of **1a** for different quenchers.

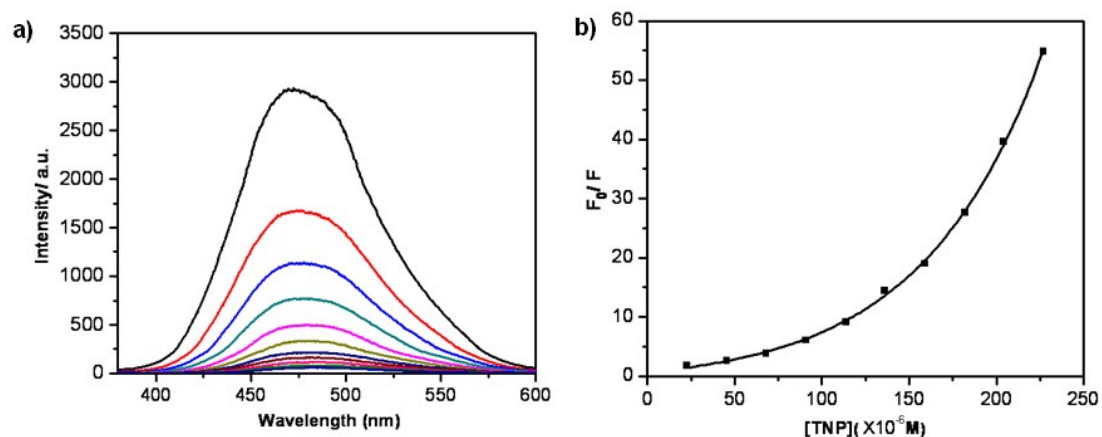


Fig. S11 (a) Emission spectra ($\lambda_{\text{ex}} = 350$ nm) of **1a** (4.5×10^{-6} M) in presence of TNP at various concentration (0, 5, 10, 15, 20, 25, 30, 35, 40, 45 and 50 equiv.). (b) The nonlinear curve-fitting for the quenching constant of **1a** with TNP.

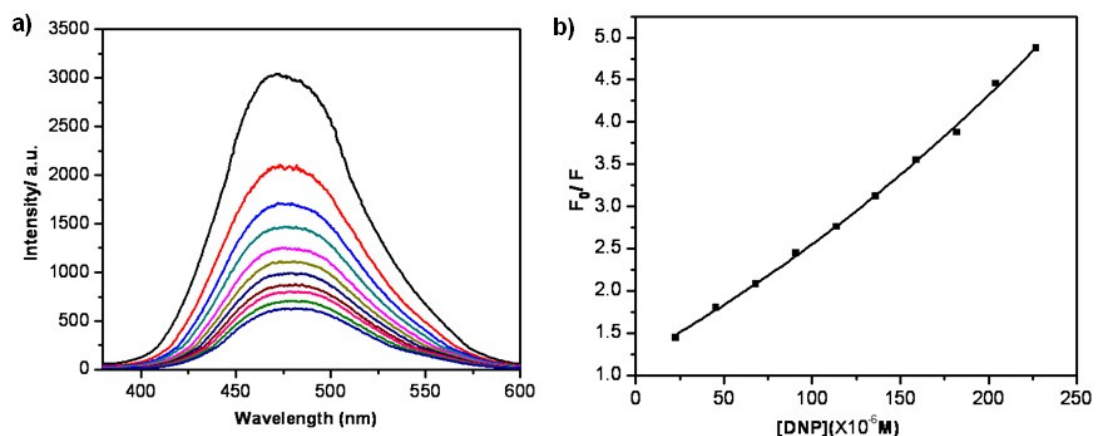


Fig.S12 (a) Emission spectra ($\lambda_{\text{ex}} = 350$ nm) of **1a** (4.5×10^{-6} M) in presence of DNP at various concentration (0, 5, 10, 15, 20, 25, 30, 35, 40, 45 and 50 equiv.). (b) The nonlinear curve-fitting for the quenching constant of **1a** with DNP.

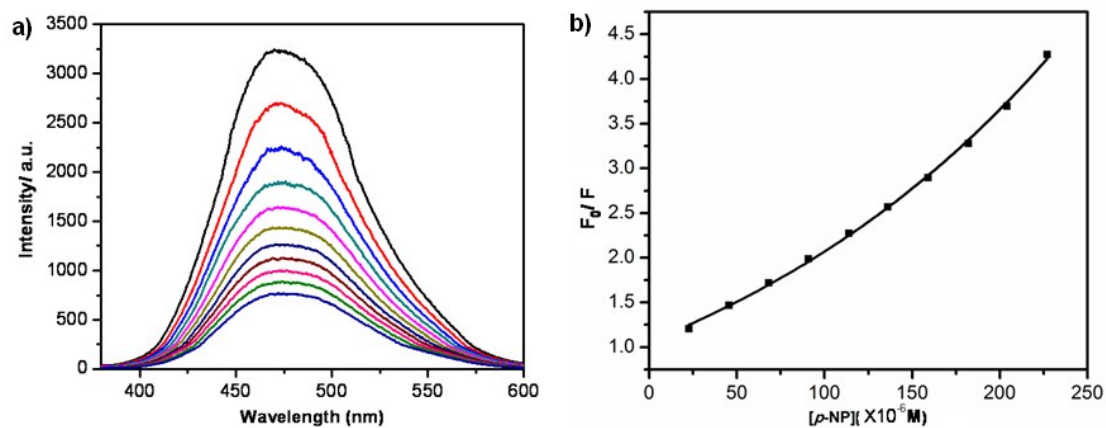


Fig. S13 (a) Emission spectra ($\lambda_{\text{ex}} = 350 \text{ nm}$) of **1a** ($4.5 \times 10^{-6} \text{ M}$) in presence of *p*-NP at various concentration (0, 5, 10, 15, 20, 25, 30, 35, 40, 45 and 50 equiv.). (b) The nonlinear curve-fitting for the quenching constant of **1a** with *p*-NP.

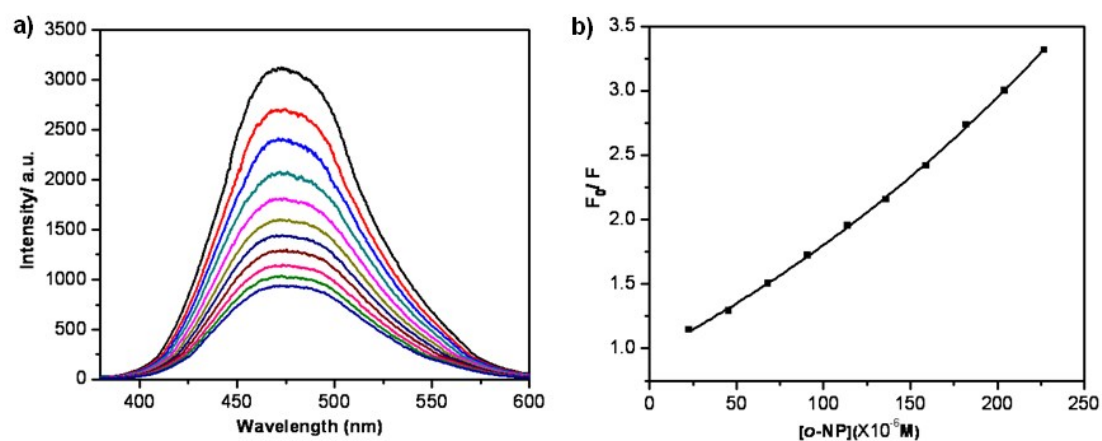


Fig. S14 (a) Emission spectra ($\lambda_{\text{ex}} = 350 \text{ nm}$) of **1a** ($4.5 \times 10^{-6} \text{ M}$) in presence of *o*-NP at various concentration (0, 5, 10, 15, 20, 25, 30, 35, 40, 45 and 50 equiv.). (b) The nonlinear curve-fitting for the quenching constant of **1a** with *o*-NP.

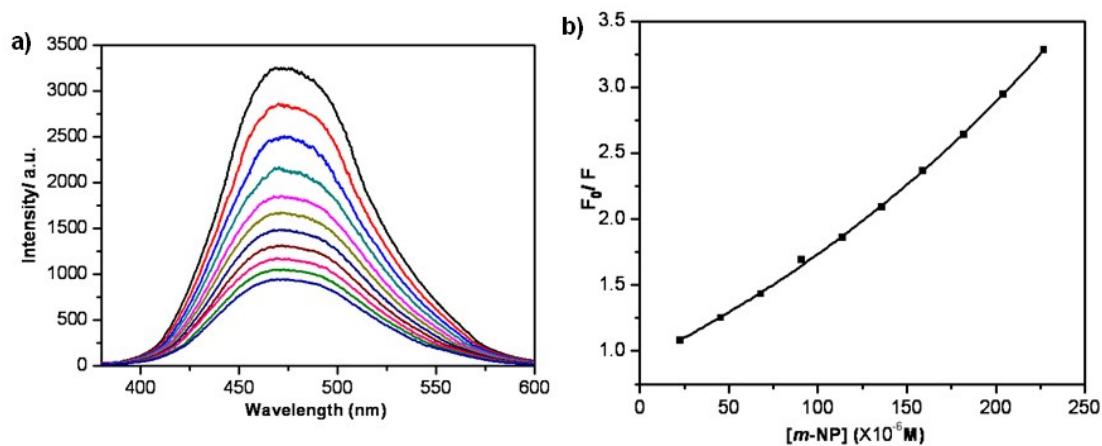


Fig. S15 (a) Emission spectra ($\lambda_{\text{ex}} = 350 \text{ nm}$) of **1a** ($4.5 \times 10^{-6} \text{ M}$) in presence of *m*-NP at various concentration (0, 5, 10, 15, 20, 25, 30, 35, 40, 45 and 50 equiv.). (b) The nonlinear curve-fitting for the quenching constant of **1a** with *m*-NP.

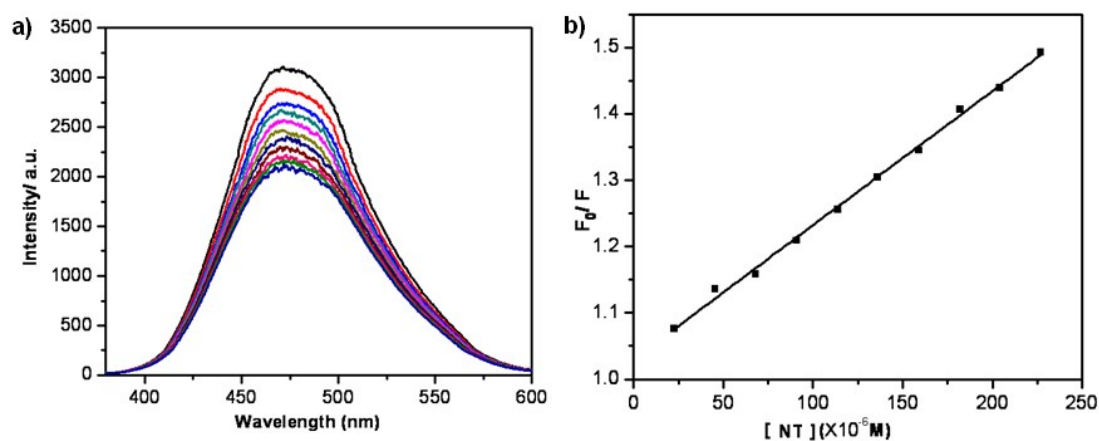


Fig. S16 (a) Emission spectra ($\lambda_{\text{ex}} = 350 \text{ nm}$) of **1a** ($4.5 \times 10^{-6} \text{ M}$) in presence of NT at various concentration (0, 5, 10, 15, 20, 25, 30, 35, 40, 45 and 50 equiv.). (b) The nonlinear curve-fitting for the quenching constant of **1a** with NT.

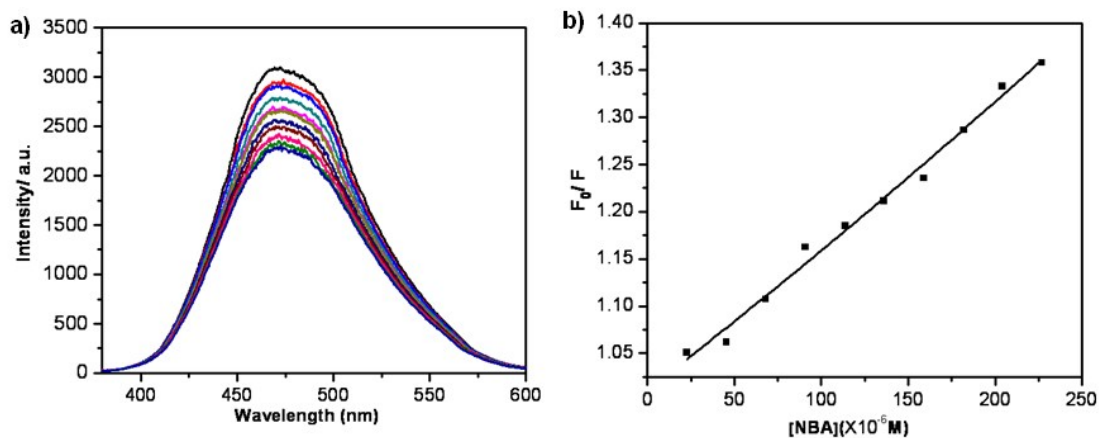


Fig. S17 (a) Emission spectra ($\lambda_{\text{ex}} = 350 \text{ nm}$) of **1a** ($4.5 \times 10^{-6} \text{ M}$) in presence of NBA at various concentration (0, 5, 10, 15, 20, 25, 30, 35, 40, 45 and 50 equiv.). (b) The nonlinear curve-fitting for the quenching constant of **1a** with NBA.

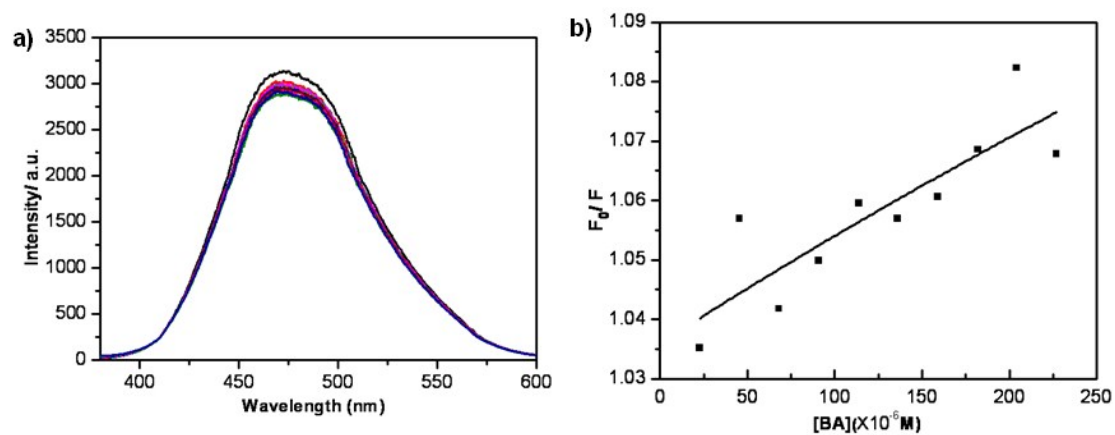


Fig S18 (a) Emission spectra ($\lambda_{\text{ex}} = 350 \text{ nm}$) of **1a** ($4.5 \times 10^{-6} \text{ M}$) in presence of BA at various concentration (0, 5, 10, 15, 20, 25, 30, 35, 40, 45 and 50 equiv.). (b) The nonlinear curve-fitting for the quenching constant of **1a** with BA.

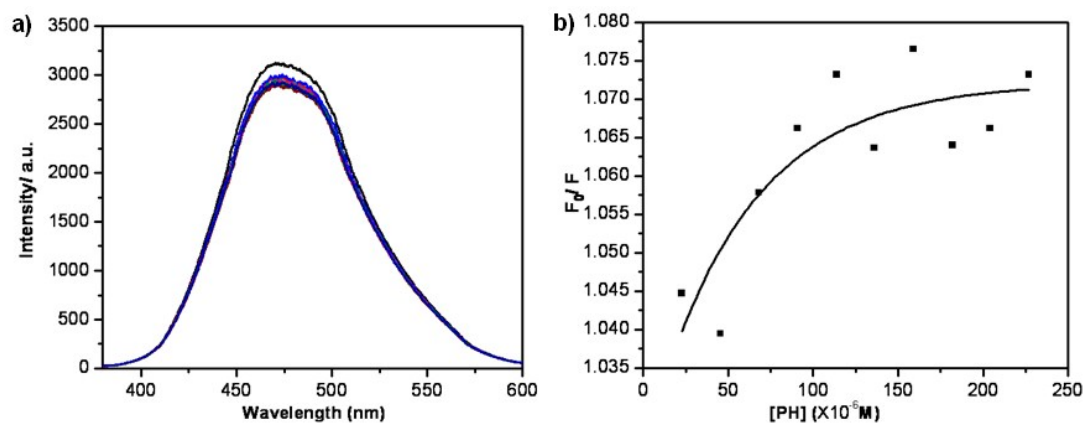


Fig. S19 (a) Emission spectra ($\lambda_{\text{ex}} = 350 \text{ nm}$) of **1a** ($4.5 \times 10^{-6} \text{ M}$) in presence of PH at various concentration (0, 5, 10, 15, 20, 25, 30, 35, 40, 45 and 50 equiv.). (b) The nonlinear curve-fitting for the quenching constant of **1a** with PH.

Table S1. Summary of fluorescence quenching constants of **1a**.

Quencher	TNP	DNP	<i>p</i> -NP	<i>o</i> -NP	<i>m</i> -NP	NT	NBA	BA	PH
K (M^{-1})	1.7×10^4	5.8×10^3	6.0×10^3	5.2×10^3	5.4×10^3	1.6×10^3	1.3×10^3	1.6×10^2	1.3×10^2

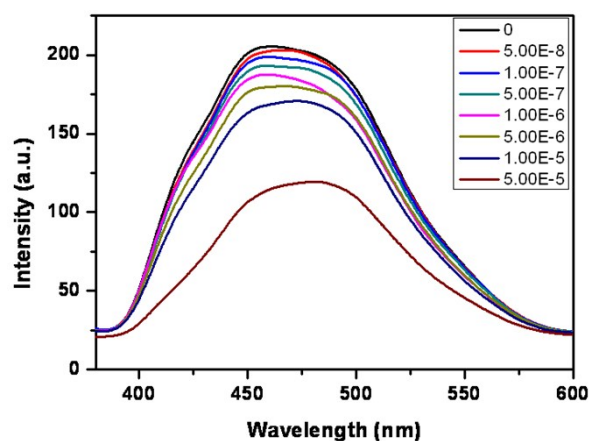


Fig. S20 Changes in the fluorescence spectra of **1a** ($5.0 \times 10^{-7} \text{ M}$) with different concentrations of TNP.